

Generative CKM Construction using Partially Observed Data with Diffusion Model

Shen Fu*, Zijian Wu*, Di Wu*[†], and Yong Zeng*[†]

*National Mobile Communications Research Laboratory, Southeast University, Nanjing 210096, China

[†]Purple Mountain Laboratories, Nanjing 211111, China

sfu@seu.edu.cn, wuzijian@seu.edu.cn, studywudi@seu.edu.cn, yong_zeng@seu.edu.cn

Abstract—Channel knowledge map (CKM) is a promising technique that enables environment-aware wireless networks by utilizing location-specific channel prior information to improve communication and sensing performance. A fundamental problem for CKM construction is how to utilize partially observed channel knowledge data to reconstruct a complete CKM for all possible locations of interest. This problem resembles the long-standing ill-posed inverse problem, which tries to infer from a set of limited observations the cause factors that produced them. By utilizing the recent advances of solving inverse problems with generative artificial intelligence (AI), in this paper, we propose generative CKM construction method using partially observed data by solving inverse problems with diffusion models. Simulation results show that the proposed method significantly improves the performance of CKM construction compared with benchmarking schemes.

Index Terms—Channel knowledge map (CKM), Generative artificial intelligence (AI), Diffusion model, inverse problem.

I. INTRODUCTION

The ever-increasing demand for efficient and reliable wireless communication drives researchers to explore innovative approaches, such as extremely large-scale multiple-input multiple-output (XL-MIMO) [1] and millimeter-wave (mmWave) communication. However, obtaining accurate and timely channel state information (CSI) in complex communication environment remains challenging [2]. To address this issue, [3] proposed the concept of channel knowledge map (CKM), which is a site-specific database, tagged with the locations of the transmitters and receivers. By enabling environment-aware communications and sensing, CKM facilitates real-time CSI acquisition, thereby promising better performance than conventional environment-unaware communications which heavily rely on real-time channel training. The significance of CKM is especially appealing for scenarios where real-time channel training is either extremely costly or infeasible in practice [4].

A fundamental problem for CKM-enabled wireless systems is how to utilize the collected location-specific channel data to construct a complete CKM. In practice, the acquisition of complete data measurements for all possible locations is costly or even impossible. Consequently, the available data are often sparse and incomplete. The authors in [5] provided analytical insights into the amount of data required for CKM construction and channel prediction. A CKM construction method based on the expectation maximization (EM) algorithm was proposed,

combining available measurement data with expert knowledge from established statistical channel models [6]. Besides, another straightforward approach is interpolation-based CKM construction, which includes K-nearest neighbors (KNN) [7], Kriging [8], and radial basis function (RBF) [9] interpolation. However, interpolation-based CKM construction presents inherent limitations, since sparse or unevenly distributed data points usually cause significant estimation errors. Furthermore, interpolation cannot inherently capture the complex physical phenomena driving channel variations, thereby restricting its ability to model intricate environments accurately.

The advancement of artificial intelligence (AI) brings new opportunities for CKM construction. The authors in [10] proposed a RadioUNet architecture which maps an image representing the buildings and transmitters to a CKM image. The authors in [11] applied a conditional generative adversarial network (cGAN) to estimate fine-resolution CKMs from sparse channel knowledge data. [12] utilized diffusion model to achieve sampling-free CKM construction with BS and environmental information as prompts. Nevertheless, all of the above methods mainly rely on physical environment data and/or transmitter location information to reconstruct CKM. Different from the above research works, we consider the problem to directly use partially observed channel knowledge data to reconstruct the complete CKM without the use of any auxiliary environmental or positional data. This approach is particularly significant as it mirrors the challenges of ill-posed inverse problems frequently encountered in computer vision.

Generative AI provides a transformative framework for tackling such problems, especially diffusion model [13], offering the capability to learn the underlying implicit data distributions. This is different from traditional methods that rely on predefined physical models or localized data, making it hard for them to understand complicated global patterns. Hence, we view the incomplete CKM images as conditions to train a conditional denoiser in decoupled diffusion model (DDM) architecture proposed in [14]. Simulation results show that for the CKMImageNet dataset [15], our method is much better than interpolation methods in terms of mean squared error (MSE) and other indicators on the inpainted CKM images.

II. SYSTEM MODEL

We consider the problem of constructing a complete CKM based on partially observed channel knowledge data for an area

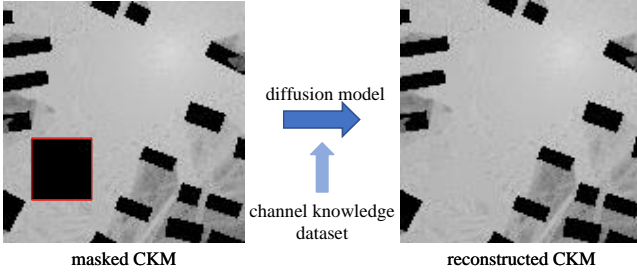


Fig. 1: CKM image inpainting task framework.

of interest. We discretize the area into $l \times w$ locations, each involving several types of channel knowledge like channel gain map, angle of arrival (AoA) map, and angle of departure (AoD) map. For each channel knowledge type, the incomplete CKM can be represented as

$$\mathbf{y} = \mathbf{H}\mathbf{x}, \quad (1)$$

where $\mathbf{y} \in \mathbb{C}^{lw \times 1}$ and $\mathbf{x} \in \mathbb{C}^{lw \times 1}$ denote the partially observed CKM and complete CKM, respectively. $\mathbf{H} \in \mathbb{C}^{lw \times lw}$ is a diagonal matrix representing the image mask, where \mathbf{H}_{ii} is either 1 and 0, based on whether the channel knowledge at this location is observed or not.

We aim to reconstruct the complete CKM, denoted as $\hat{\mathbf{x}}$, from its partially observed counterpart \mathbf{y} . This is a classical linear inverse problem. A straightforward approach to address this problem is maximizing the posterior distribution $q(\mathbf{x}|\mathbf{y})$, where $q(\mathbf{x}|\mathbf{y}) \propto q(\mathbf{y}|\mathbf{x})q(\mathbf{x})$. However, in scenarios where the prior distribution $q(\mathbf{x})$ is unknown, the problem becomes underdetermined due to the rank-deficiency of the mask matrix \mathbf{H} . This rank-deficiency results in the existence of multiple plausible solutions that satisfy the given observations, making the reconstruction task inherently ill-posed. One naive method is to compute the pseudo-inverse of \mathbf{H} , which gives the least-squares solution as $\hat{\mathbf{x}} = \mathbf{H}^\dagger \mathbf{y}$, where \mathbf{H}^\dagger denotes the pseudo-inverse of \mathbf{H} . However, this approach usually gives poor performance. Besides, interpolation techniques can also be applied to complete partially missing data, such as linear, bilinear and Kriging interpolation. But various interpolation methods may result in low-quality outcomes, as they often estimate missing data values solely based on the known values surrounding them.

The core concept of the proposed approach focuses on effectively learning the prior distribution $q(\mathbf{x})$, which aligns seamlessly with the principles of generative diffusion models in [13]. By leveraging diffusion model trained on a dataset $\{\mathbf{x}\}$, the method captures the intricate relationships and underlying structures within the data. This enables the reconstruction of missing information in CKMs, as illustrated in Fig. 1.

III. CKM CONSTRUCTION VIA DIFFUSION MODELS

A. Principles of Diffusion Models

The core principle of denoising diffusion probabilistic models (DDPM), proposed in [13], is to model the data distribution $q(\mathbf{x})$ by minimizing a variational bound on the negative log-likelihood. This framework utilizes a forward process to

gradually corrupt the data by adding Gaussian noise over a sequence of time steps $t \in [1, T]$, and a reverse process to reconstruct the original data by denoising step-by-step. Starting from an initial data \mathbf{x}_0 , the forward process is defined as:

$$q(\mathbf{x}_t|\mathbf{x}_{t-1}) = \mathcal{N}\left(\mathbf{x}_t; \sqrt{1 - \beta_t}\mathbf{x}_{t-1}, \beta_t\mathbf{I}\right), \quad (2)$$

where β_t is a variance schedule that determines how much noise is added at each step t , and \mathbf{I} is the identity matrix. The process is continued until time step T , when the original data are completely corrupted by noise. It is known that the forward process admits sampling \mathbf{x}_t at an arbitrary timestep t in closed form:

$$q(\mathbf{x}_t|\mathbf{x}_0) = \mathcal{N}\left(\mathbf{x}_t; \sqrt{\bar{\alpha}_t}\mathbf{x}_0, (1 - \bar{\alpha}_t)\mathbf{I}\right), \quad (3)$$

where $\bar{\alpha}_t = \prod_{s=1}^t \alpha_s$ and $\alpha_t = 1 - \beta_t$.

The reverse process is opposite of the forward diffusion process, which aims to recover the original data by eliminating the added noise gradually. By defining a Markov chain, it starts with the highly noisy data \mathbf{x}_T and moves in reverse to \mathbf{x}_0 . The specific process from \mathbf{x}_t to \mathbf{x}_{t-1} can be expressed by

$$p_\theta(\mathbf{x}_{t-1}|\mathbf{x}_t) = \mathcal{N}\left(\mathbf{x}_{t-1}; \boldsymbol{\mu}_\theta(\mathbf{x}_t, t), \boldsymbol{\Sigma}_\theta(\mathbf{x}_t, t)\right). \quad (4)$$

Here, $\boldsymbol{\mu}_\theta$ and $\boldsymbol{\Sigma}_\theta$ are learned functions parameterized by θ . Specifically, $\boldsymbol{\mu}_\theta$ predicts the mean of the Gaussian distribution and $\boldsymbol{\Sigma}_\theta$ defines the covariance matrix.

The goal of training a diffusion model is to minimize the distance between the real data distribution and the generated data distribution. It has been shown that minimizing the variational bound on the negative log likelihood can be simplified to minimizing [13]

$$\mathcal{L} = \mathbb{E}_{t, \mathbf{x}_0, \epsilon} \left[\|\epsilon - \epsilon_\theta(\mathbf{x}_t, t)\|^2 \right], \quad (5)$$

where $\epsilon \sim \mathcal{N}(\mathbf{0}, \mathbf{I})$ is sampled noise added at each forward diffusion step, and $\mathbf{x}_t = \sqrt{\bar{\alpha}_t}\mathbf{x}_0 + \sqrt{1 - \bar{\alpha}_t}\epsilon$. A UNet structured neural network $\epsilon_\theta(\mathbf{x}_t, t)$ is applied to predict the noise.

B. Conditional Diffusion Model for CKM Inpainting

In order to further improve the quality and speed of CKM reconstruction, we apply conditional DDM proposed in [14] to solve this inverse problem. Different from DDPM, DDM converts the normal image-to-noise forward diffusion process into two stages: (i) attenuate the image component by an image-to-zero mapping, (ii) increase the noise component by a zero-to-noise mapping. By utilizing decoupled diffusion strategy, the forward diffusion process is represented by

$$\mathbf{x}_t = \mathbf{x}_0 + \int_0^t \mathbf{f}_t dt + \int_0^t d\mathbf{w}_t, \quad (6)$$

where $\mathbf{x}_0 + \int_0^t \mathbf{f}_t dt$ denotes the image attenuation process and $\int_0^t d\mathbf{w}_t$ represents the noise enhancement process. \mathbf{w}_t is the standard Wiener process, and \mathbf{f}_t is a differentiable function of t that allows arbitrary sampling steps, thus accelerating the sampling process. In this paper, we set \mathbf{f}_t as a simple but effective function $\mathbf{f}_t = \mathbf{c}$. Note that t takes the range $[0, 1]$, different from DDPM. To achieve the forward diffusion process from \mathbf{x}_0 to noise, we need to ensure that the transformation effectively transitions the initial state into a noise-dominated state. Thus,

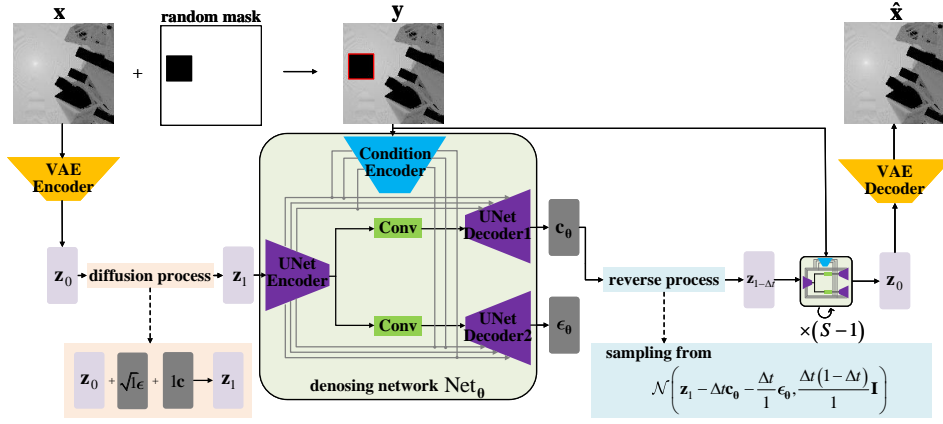


Fig. 2: Conditional decoupled diffusion model for generative CKM construction.

\mathbf{x}_0 follows the distribution $q(\mathbf{x}_0)$ and $\mathbf{x}_0 + \int_0^1 \mathbf{f}_t dt = \mathbf{0}$, satisfying that \mathbf{x}_1 is distributed as $\mathcal{N}(\mathbf{0}, \mathbf{I})$. In other words, $\mathbf{c} = -\mathbf{x}_0$.

Concisely, the forward process can be rewritten as:

$$q(\mathbf{x}_t | \mathbf{x}_0) = \mathcal{N}\left(\mathbf{x}_t; \mathbf{x}_0 + \int_0^t \mathbf{c} dt, t\mathbf{I}\right). \quad (7)$$

Therefore, we can sample \mathbf{x}_t by $\mathbf{x}_t = (1-t)\mathbf{x}_0 + \sqrt{t}\boldsymbol{\epsilon}$, where $\boldsymbol{\epsilon} \sim \mathcal{N}(\mathbf{0}, \mathbf{I})$.

Unlike DDPM which uses discrete time Markov chain, the reverse process in DDM employs continuous-time Markov chain with the smallest time step $\Delta t \rightarrow 0^+$ and we use conditional distribution $q(\mathbf{x}_{t-\Delta t} | \mathbf{x}_t, \mathbf{x}_0)$ to approximate $q(\mathbf{x}_{t-\Delta t} | \mathbf{x}_t)$:

$$q(\mathbf{x}_{t-\Delta t} | \mathbf{x}_t, \mathbf{x}_0) = \mathcal{N}\left(\mathbf{x}_t - \Delta t \mathbf{c} - \frac{\Delta t}{\sqrt{t}} \boldsymbol{\epsilon}, \frac{\Delta t(t-\Delta t)}{t} \mathbf{I}\right). \quad (8)$$

From the reverse process in (8), signal attenuation term $-\Delta t \mathbf{c}$ and noise term $\boldsymbol{\epsilon}$ are unknown. Hence, we use $p_\theta(\mathbf{x}_{t-\Delta t} | \mathbf{x}_t)$ to approximate $q(\mathbf{x}_{t-\Delta t} | \mathbf{x}_t, \mathbf{x}_0)$ and predict simultaneously \mathbf{c} and $\boldsymbol{\epsilon}$ by utilizing a modified UNet architecture Net_θ , where two stacked convolutional layers are added to create two UNet decoder branches. In addition, an encoder is employed to extract multi-level features of masked image \mathbf{y} as $e(\mathbf{y})$ for a conditional DDM to inpaint CKM images. Therefore, $p_\theta(\mathbf{x}_{t-\Delta t} | \mathbf{x}_t, e(\mathbf{y}))$ can be expressed as (9). Accordingly, the training objective is

$$\min_{\theta} \mathbb{E}_{t, \mathbf{x}_0, \boldsymbol{\epsilon}, \mathbf{y}} \left[\|\mathbf{c} - \mathbf{c}_\theta(\mathbf{x}_t, t | e(\mathbf{y}))\|^2 + \|\boldsymbol{\epsilon} - \boldsymbol{\epsilon}_\theta(\mathbf{x}_t, t | e(\mathbf{y}))\|^2 \right]. \quad (10)$$

To sum up, the specific training and sampling procedures for CKM construction are summarized in Algorithm 1 and Algorithm 2, respectively. The architecture of the network is demonstrated in Fig. 2. A variational autoencoder (VAE) is employed to map the pixel space \mathbf{x} to the latent space \mathbf{z} , aiming to reduce computational requirements and training time. Besides, we apply a Swin-B encoder [16] to extract multi-level features of the conditioned input, and concatenate these features with the image features at the UNet decoder's input levels.

Algorithm 1 The training algorithm for CKM construction

- 1: **Initialize:** $i = 0$, number of iterations: N , network parameters: θ
 - 2: **while** $i < N$ **do**
 - 3: $t \sim \text{Uniform}(0, 1)$, $\mathbf{x}_0 \sim q(\mathbf{x}_0)$, $\mathbf{c} = -\mathbf{x}_0$, $\mathbf{y} = \mathbf{H}\mathbf{x}_0$ where \mathbf{H} is a random mask matrix, $\boldsymbol{\epsilon} \sim \mathcal{N}(\mathbf{0}, \mathbf{I})$
 - 4: $e(\mathbf{y}) = \text{encoder}(\mathbf{y})$
 - 5: $\mathbf{x}_t = \mathbf{x}_0 + t\mathbf{c} + \sqrt{t}\boldsymbol{\epsilon}$
 - 6: $\mathbf{c}_\theta, \boldsymbol{\epsilon}_\theta = \text{Net}_\theta(\mathbf{x}_t, t, e(\mathbf{y}))$
 - 7: **Take gradient descent step on**
 $\nabla_{\theta} \left(\|\mathbf{c} - \mathbf{c}_\theta(\mathbf{x}_t, t | e(\mathbf{y}))\|^2 + \|\boldsymbol{\epsilon} - \boldsymbol{\epsilon}_\theta(\mathbf{x}_t, t | e(\mathbf{y}))\|^2 \right)$
 - 8: $i = i + 1$
 - 9: **end while**
 - 10: **return** θ
-

Algorithm 2 The sampling algorithm for CKM construction

- 1: **Initialize:** $\mathbf{x}_1 \sim \mathcal{N}(\mathbf{0}, \mathbf{I})$, \mathbf{y} , number of sampling steps: S , sampling interval: $\Delta t = 1/S$, Net_θ
 - 2: **while** $t > 0$ **do**
 - 3: $\tilde{\boldsymbol{\epsilon}} \sim \mathcal{N}(\mathbf{0}, \mathbf{I})$
 - 4: $e(\mathbf{y}) = \text{encoder}(\mathbf{y})$
 - 5: $\mathbf{c}_\theta, \boldsymbol{\epsilon}_\theta = \text{Net}_\theta(\mathbf{x}_t, t, e(\mathbf{y}))$
 - 6: $\mathbf{x}_t = \mathbf{x}_t - \Delta t \mathbf{c}_\theta - \frac{\Delta t}{\sqrt{t}} \boldsymbol{\epsilon}_\theta + \sqrt{\frac{\Delta t(t-\Delta t)}{t}} \tilde{\boldsymbol{\epsilon}}$
 - 7: $t = t - \Delta t$
 - 8: **end while**
 - 9: **return** \mathbf{x}_t
-

IV. NUMERICAL RESULTS

A. Dataset and Simulation Setup

The CKMImageNet dataset is used to train and verify our model [15]. The CKMImageNet dataset is a mixed dataset of numerical data, images of different resolutions and environment maps. The data are obtained from ray-tracing by using commercial software *Wireless Insite*¹, which simulates electromagnetic wave propagation with high fidelity as it models the interactions of waves with the environment, including reflections, diffractions, and scatterings. Specifically,

$$p_{\theta}(\mathbf{x}_{t-\Delta t}|\mathbf{x}_t, e(\mathbf{y})) = \mathcal{N}\left(\mathbf{x}_{t-\Delta t}; \mathbf{x}_t - \Delta t \mathbf{c}_{\theta}(\mathbf{x}_t, t|e(\mathbf{y})) - \frac{\Delta t}{\sqrt{t}} \boldsymbol{\epsilon}_{\theta}(\mathbf{x}_t, t|e(\mathbf{y})), \frac{\Delta t(t-\Delta t)}{t} \mathbf{I}\right). \quad (9)$$

six reflections and one diffraction were configured for the CKMImageNet dataset. The simulation settings involve a transmit power of 0 dBm and a carrier frequency of 28 GHz, with the transmitter and receiver heights set to 10 meters and 1 meter, respectively. The environment map involves cities like Beijing, Shanghai, London, etc, and the city maps are mainly provided by *OpenStreetMap*². Currently, the CKMImageNet dataset consists of over 30000 images of the resolution of 128×128 , where adjacent pixel points are spaced two meters apart in the real-world terrain. As for the channel gain images, the channel gain values are between -50dB and -250dB , and the values are linearly mapped to $[0, 255]$ to form the grayscale images that the diffusion model requires. In addition, we assume that the values in areas where there are buildings are the minimum value of -250 , which is map to gray scale 0 and shows black in grayscale image.

We use 20000 128×128 channel gain images as training dataset, and 2000 channel gain images as testing dataset. We train our CKM image inpainting model in two steps. First, a VAE is trained to map the pixel space to the latent space. An AdamW optimizer is utilized with a scheduled learning rate from $5e-6$ to $1e-6$. Next, we train a conditional DDM using the AdamW optimizer. The model is trained for 300,000 iterations with a batch size of 48 and the smallest time step is 1×10^4 . All the above training and sampling processes can be implemented on a NVIDIA GeForce RTX 4090.

B. Simulation Results

We complete CKM images for two scenarios: mask covers the buildings and mask does not cover the buildings. Besides, to better illustrate the effectiveness of CKM reconstruction, we convert pixel values in gray images into CKM ground truth values and further calculate error metrics for all locations without building occupancy, i.e., MSE, normalized MSE (NMSE), root MSE (RMSE) and mean absolute error (MAE).

Fig. 3 illustrates the inpainting effect of the scenario where the mask covers the buildings. Here we compare our method with several interpolation methods, such as KNN, Kriging, Bilinear [17] and RBF interpolation. Table I plots the average error metrics of inpainting 1000 CKM images when masking buildings with the five methods. It is observed that our proposed diffusion based model significantly outperforms significantly the benchmark approaches.

Fig. 4 demonstrates the visualization examples of CKM images inpainting task when the buildings are not masked. The error metrics comparison of the considered methods to test 500 CKM images are listed in Table II. The reconstruction error of our proposed scheme is the smallest in comparison with the four benchmarking methods, with a RMSE of 10.7758 dB

TABLE I: Performance Comparison With Masking Buildings

	KNN	Kriging	Bilinear	RBF	Proposed
MSE(dB ²)	4359.266	1868.018	3526.219	2910.859	427.299
NMSE	0.0722	0.0309	0.0584	0.0482	0.0071
RMSE(dB)	66.0247	43.2206	59.3820	53.9524	20.6712
MAE(dB)	36.7986	29.8942	40.2318	34.0901	9.9813

TABLE II: Performance Comparison Without Masking Buildings

	KNN	Kriging	Bilinear	RBF	Proposed
MSE(dB ²)	245.7755	272.5737	474.6037	188.2536	116.1187
NMSE	0.0041	0.0046	0.0079	0.0032	0.0019
RMSE(dB)	15.6772	16.5098	21.7854	13.7206	10.7758
MAE(dB)	5.8437	8.5845	8.0328	6.0715	5.1412

TABLE III: Performance Comparison When Masking BS

	KNN	Kriging	Bilinear	RBF	Proposed
MSE(dB ²)	42.4357	825.4937	45.5672	212.3440	27.3767
NMSE	0.0007	0.0138	0.0008	0.0035	0.0005
RMSE(dB)	6.5143	28.7314	6.7503	14.5720	5.2323
MAE(dB)	2.6440	13.0177	2.6920	4.6491	2.1114
BS loc. err.(m)	8.81	9.12	8.88	13.71	3.30

and a MAE of 5.1412 dB. Besides, in contrast to Table I, the completion effect when buildings are not covered is significantly better for all schemes.

It is worth mentioning that our proposed approach is also quite effective for base station (BS) localization in complex environment. Specifically, we consider the channel knowledge of the $64\text{m} \times 64\text{m}$ area including the BS in the real physical environment within the range of $256\text{m} \times 256\text{m}$ is missing, whose visualization effects of different methods for CKMImageNet dataset is shown in Fig. 5. Table III lists the error indicators in predicting channel knowledge of the BS's vicinity and the BS localization error for five schemes, where the testing dataset size is 1000. Note that the diffusion model is much better than the interpolation methods in predicting the channel knowledge near the BS and the positioning performance of the BS. Compared with the BS position in the ground truth, the positioning error is only 3.30m even in complex urban environment without LoS links in most cases.

V. CONCLUSION

In this paper, we proposed a novel generative CKM construction method based on conditional diffusion models with partially observed channel knowledge data. Simulation results demonstrate the effectiveness of the proposed method across two different scenarios: masking buildings and not masking

¹<https://www.remcom.com/wireless-insite-em-propagation-software>

²<https://www.openstreetmap.org/>

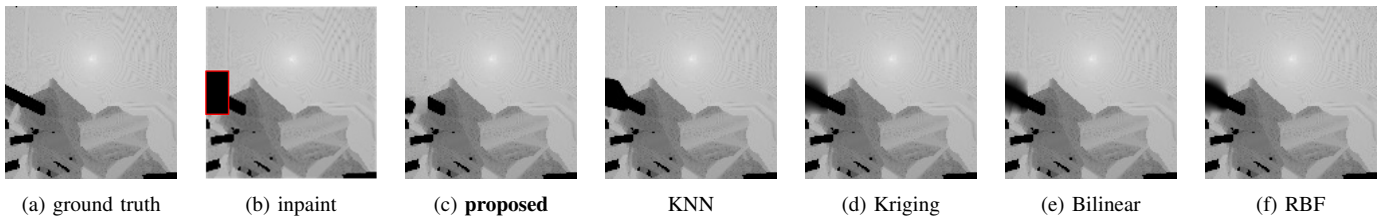


Fig. 3: Visualization results of different methods when buildings are masked.

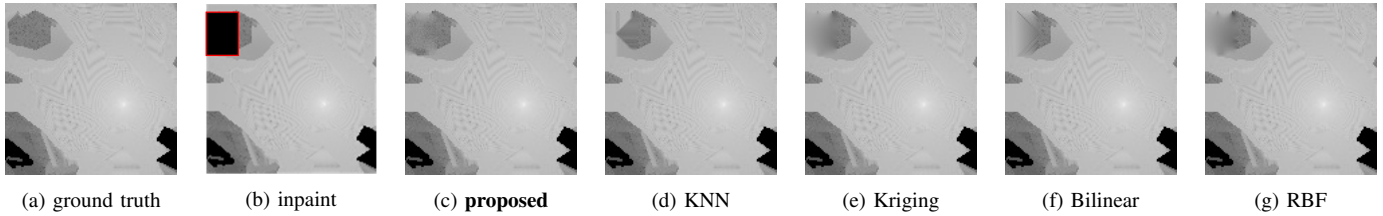


Fig. 4: Visualization results of different methods without masking buildings.

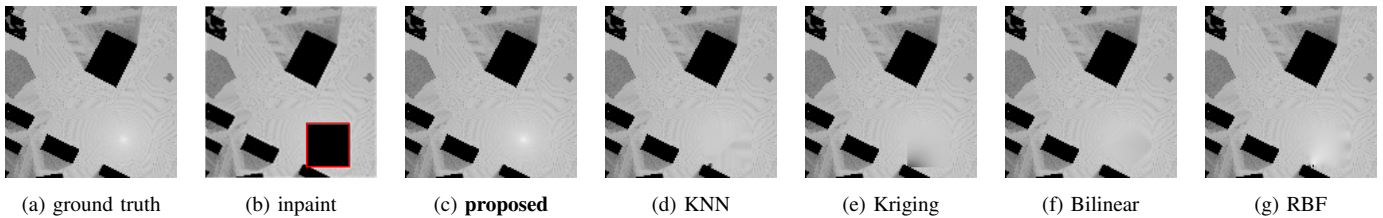


Fig. 5: Visualization results of different methods to localize the BS.

buildings. Additionally, our proposed method for BS localization achieves superior performance on the CKMImageNet dataset, outperforming benchmark methods.

REFERENCES

- [1] H. Lu, Y. Zeng, C. You, Y. Han, J. Zhang, Z. Wang, Z. Dong, S. Jin, C.-X. Wang, T. Jiang *et al.*, “A tutorial on near-field XL-MIMO communications towards 6G,” *IEEE Commun. Surv. Tutorials*, 2024.
- [2] V. Venkateswaran and A.-J. van der Veen, “Analog beamforming in MIMO communications with phase shift networks and online channel estimation,” *IEEE Trans. Signal Process.*, vol. 58, no. 8, pp. 4131–4143, 2010.
- [3] Y. Zeng and X. Xu, “Toward environment-aware 6G communications via channel knowledge map,” *IEEE Wireless Commun.*, vol. 28, no. 3, pp. 84–91, 2021.
- [4] Y. Zeng, J. Chen, J. Xu, D. Wu, X. Xu, S. Jin, X. Gao, D. Gesbert, S. Cui, and R. Zhang, “A tutorial on environment-aware communications via channel knowledge map for 6G,” *IEEE Commun. Surv. Tutorials*, pp. 1–1, 2024.
- [5] X. Xu and Y. Zeng, “How much data is needed for channel knowledge map construction?” *IEEE Trans. Wireless Commun.*, vol. 23, no. 10, pp. 13 011–13 021, 2024.
- [6] K. Li, P. Li, Y. Zeng, and J. Xu, “Channel knowledge map for environment-aware communications: EM algorithm for map construction,” in *2022 IEEE Wireless Commun. and Networking Conf. (WCNC)*, 2022, pp. 1659–1664.
- [7] S. Sun and R. Huang, “An adaptive k-nearest neighbor algorithm,” in *2010 Seventh Int. Conf. Fuzzy Syst. Knowl. Discov.*, vol. 1, 2010, pp. 91–94.
- [8] H. Braham, S. B. Jemaa, G. Fort, E. Moulines, and B. Sayrac, “Fixed rank kriging for cellular coverage analysis,” *IEEE Trans. Veh. Technol.*, vol. 66, no. 5, pp. 4212–4222, 2017.
- [9] X. Chai and Q. Yang, “Reducing the calibration effort for probabilistic indoor location estimation,” *IEEE Trans. Mobile Comput.*, vol. 6, no. 6, pp. 649–662, 2007.
- [10] R. Levie, Ç. Yapar, G. Kutyniok, and G. Caire, “Radiounet: Fast radio map estimation with convolutional neural networks,” *IEEE Trans. Wireless Commun.*, vol. 20, no. 6, pp. 4001–4015, 2021.
- [11] S. Zhang, A. Wijesinghe, and Z. Ding, “RME-GAN: A learning framework for radio map estimation based on conditional generative adversarial network,” *IEEE Internet Things J.*, vol. 10, no. 20, pp. 18 016–18 027, 2023.
- [12] X. Wang, K. Tao, N. Cheng, Z. Yin, Z. Li, Y. Zhang, and X. Shen, “Radiodiff: An effective generative diffusion model for sampling-free dynamic radio map construction,” *IEEE Trans. Cogn. Commun. Networking*, 2024.
- [13] J. Ho, A. Jain, and P. Abbeel, “Denoising diffusion probabilistic models,” *Adv. Neural Inf. Process. Syst. (NeurIPS)*, vol. 33, pp. 6840–6851, 2020.
- [14] Y. Huang, Z. Qin, X. Liu, and K. Xu, “Decoupled diffusion models: Simultaneous image to zero and zero to noise,” *arXiv preprint arXiv:2306.13720*, 2023.
- [15] D. Wu, Z. Wu, Y. Qiu, S. Fu, and Y. Zeng, “CKMImageNet: A comprehensive dataset to enable channel knowledge map construction via computer vision,” in *2024 IEEE/CIC Int. Conf. Commun. China (ICCC Workshops)*, 2024, pp. 114–119.
- [16] Z. Liu, Y. Lin, Y. Cao, H. Hu, Y. Wei, Z. Zhang, S. Lin, and B. Guo, “Swin transformer: Hierarchical vision transformer using shifted windows,” in *Proc. IEEE/CVF Int. Conf. Comput. Vis. (ICCV)*, 2021, pp. 10 012–10 022.
- [17] E. J. Kirkland and E. J. Kirkland, “Bilinear interpolation,” *Adv. Comput. Electron Microsc.*, pp. 261–263, 2010.